CONF-08-425-AD

STABILITY OF ELECTRON ENERGY IN THE FERMILAB ELECTRON COOLER*

A. Shemyakin[#], K. Carlson, , L.R. Prost, G. Saewert
FNAL, Batavia, IL 60510, U.S.A.
February 12, 2009

Abstract. A powerful electron beam (4.3 MeV, 0.1 A DC) generated by an electrostatic accelerator has been used at Fermilab for three years to cool antiprotons in the Recycler ring. For electron cooling to be effective, the electron energy should not deviate from its optimum value by more than 500V. The main tool for studying the energy stability is the electron beam position in a high-dispersion area. The energy ripple (frequencies above 0.2 Hz) was found to be less than 150 eV rms; the main cause of the ripple is the fluctuations of the chain current. In addition, the energy can drift to up to several keV that is traced to two main sources. One of them is a drift of the charging current, and another is a temperature dependence of generating voltmeter readings. The paper describes the efforts to reach the required level of stability as well as the setup, diagnostics, results of measurements, and operational experience.

Keywords: Electron cooling, electrostatic accelerator, electron beam
PACS: 29.17.+w, 29.25.Bx, 29.27.Eg, 41.75.Ht

1. INTRODUCTION

Electron cooling [1] is a process of decreasing emittances of heavy-particle beams (ions or antiprotons) through the Coulomb scattering of the "hot" heavy particles in a "cold" electron gas when the beams co-propagate with the same velocity in a common region called the cooling section. Since its first successful test in 1975 [2], electron cooling has been used at dozens of storage rings [3] in the keV- range of the electron energy. However, relativistic electron cooling was demonstrated only at Fermilab in July 2005 [4]. Shortly after, the Recycler Electron Cooler began to be used around the clock in routine operation to accumulate antiprotons in the Recycler ring and prepare them for shots to the Tevatron collider [5].

One of the challenges during commissioning of the cooler and its routine operation was to match the velocities of the antiproton and electron beams in the cooling section. Efficiency of electron cooling drops significantly if the electron energy deviates from the optimum by more than 500 eV. Because the beam is generated by a 5-MV

* FNAL is operated by Fermi Research Alliance, LLC under Contract No. DE-AC02-07CH11359 with the United States Department of Energy.
[#]shemyakin@fnal.gov

electrostatic accelerator, a Pelletron [6], this restriction means stabilization of the terminal voltage to the level of 0.01%.

Pelletrons have been reported as capable of very good voltage stability and low ripple. For example, Ref.[7] reported a ripple of 0.003%; Ref. [8] mentions operation for days with the high voltage reported by a generating voltmeter being stable at the 0.01% level. With ion accelerators, which most of the Pelletrons are, the absolute energy calibration and test of energy stability can be done with the use of nuclear reactions. Such a test described in Ref. [9] suggests that the long-term stability of the Pelletron's terminal voltage can be improved to the 0.003% level. For electron machines, we can refer to the experience of UCSB's free electron laser system, where a Pelletron is used to generate the electron beam. The lasing characteristics suggest that the energy stability was better than 0.05% [10].

Efforts to find and maintain the optimal energy in the Recycler Electron Cooler are the subject of this paper. We describe the setup in Section 1 and the diagnostics in Section 2; Section 3 is devoted to the discussion of energy regulation loops; Section 4 presents the current energy stability performance; in Section 5 we are discussing operational issues related to this stability, and then conclude. Appendix A contains the list of the abbreviations which were used throughout the paper.

2. SETUP DESCRIPTION

The mechanical schematic of the Electron Cooler is shown in Fig.2.1. The electron beam is generated by an electrostatic accelerator, the Pelletron, and transported through a beam "supply" line to the cooling section where it interacts with antiprotons circulating in the Recycler ring. After separation of the beams by a 180 degree bend magnet, electrons move through the "return" and "transfer" beam lines back to the Pelletron, are decelerated in the second Pelletron tube, and the beam is absorbed in a collector at the kinetic energy of 3.2 keV. Some of the cooler parameters are listed in Table 2.1.

The vacuum chamber is pumped down by ion and titanium sublimation pumps. The typical diameter of the beam line vacuum chamber is 75 mm, but the aperture is limited by the BPM's inner diameter of 47 mm.

When both main bending magnets under the Pelletron are turned off, the beam can be recirculated through a short beam line, denoted as U-bend in Fig.2.1. This so-called U- bend mode was used for commissioning purposes. For instance, in this mode we were able to reach DC beam currents of up to 1.8 A at the nominal energy.

Table 2.1. Some parameters of the cooler.

Parameter	**Unit**	**Value**
Electron energy	MeV	4.338
Beam current used for cooling	A	0.1 - 0.5
Maximum DC beam current	A	0.7
Magnetic field in the cooling section	G	105
Beam radius in the cooling section	mm	2.5
Pressure	nTorr	0.2 - 1
Total length of the beam line	m	90

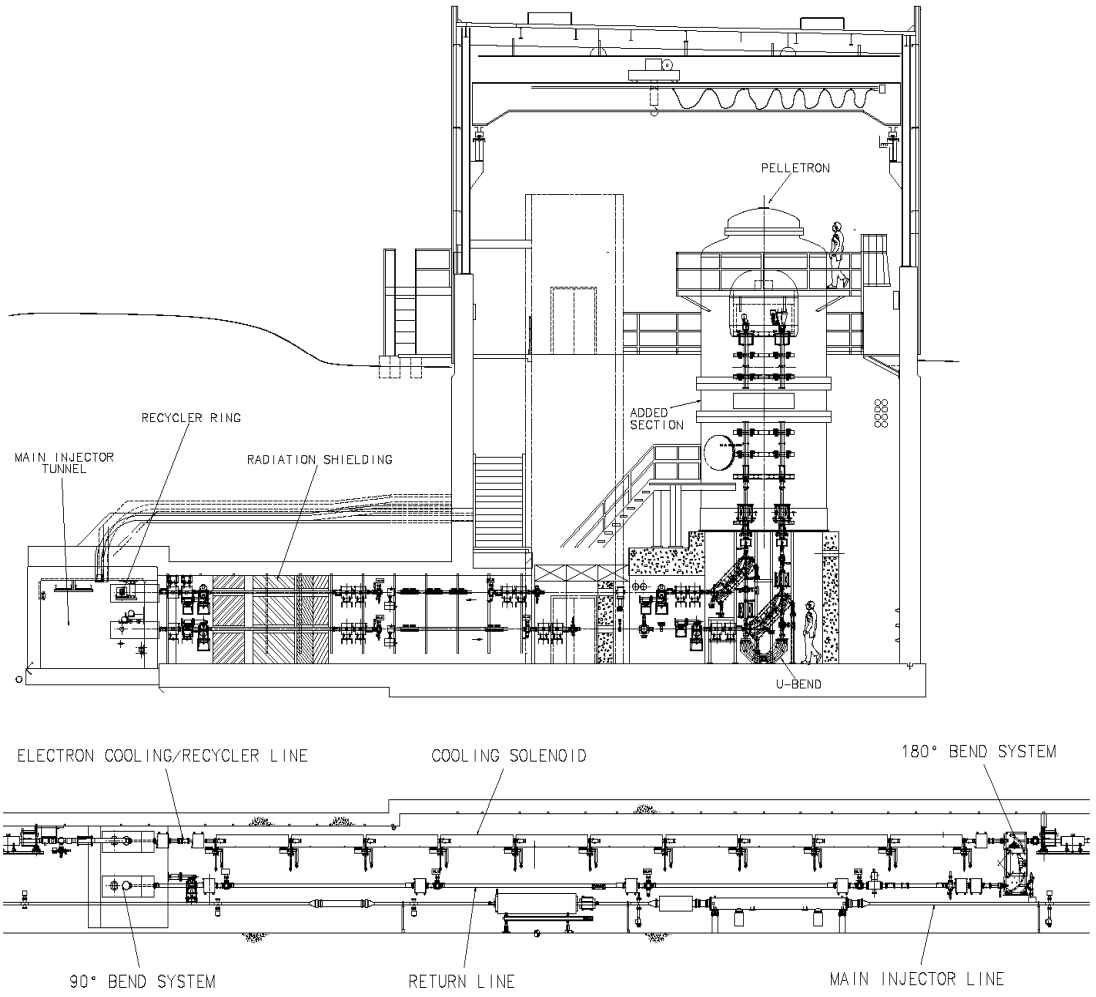

FIGURE 2.1. The top insert is an elevation view showing the Pelletron, the acceleration and deceleration beam lines, the transfer lines passing through a connecting enclosure to the Recycler ring, and the cross-section of the MI tunnel which houses the Recycler ring and the 150 GeV synchrotron Main Injector. The distance between the axes of the acceleration and deceleration tubes is 1 m. The bottom insert is an elevation view of the MI tunnel showing the 90°-bend system which injects the electron beam from the transfer line into the Recycler ring, the cooling section of Recycler, the 180°-bend system which extracts the electron beam from the Recycler, and the return line. The distance between the axes of the cooling section and the return line is 1 m.

A simplified electrical schematic of the accelerator is shown in Fig.2.2. Typically, the Pelletron chain supplies 110 μA, from which 95 μA go to the resistive strings and 15 μA are used to provide the voltage stabilization and compensation of the beam loss.

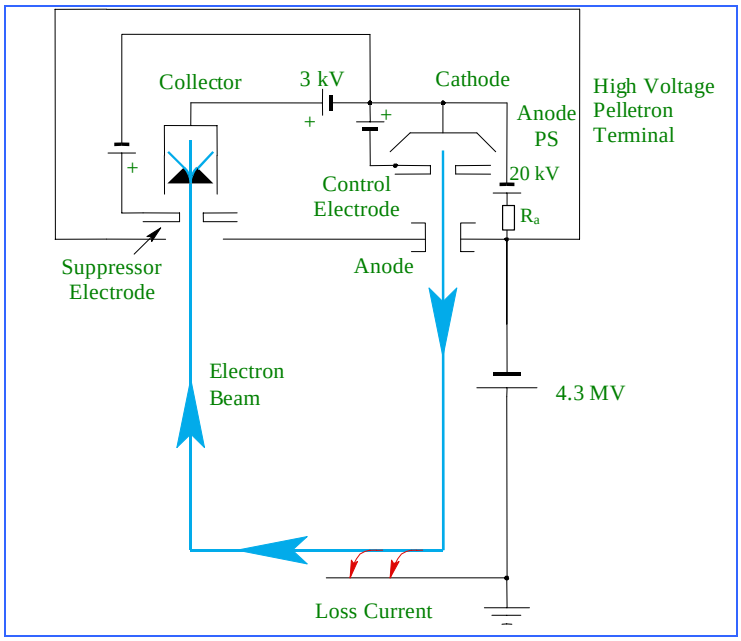

Figure 2.2. Simplified electrical schematic of the accelerator showing the recirculation scheme.

The cooler is controlled through a Fermilab-wide control system called ACNET. ACNET interacts with the Pelletron through a system called ACCELNET, which is provided by the manufacturer, NEC.

3. RELEVANT DIAGNOSTICS

The electron energy and its deviations are measured either by measuring the voltage of the terminal or by analyzing the beam trajectory. To measure the terminal high voltage (HV), the Pelletron is equipped with a Generating Volt Meter (GVM) and two capacitive pickups (or Capacitive Pick-Outs, CPO), which are located in the pressure vessel walls and facing the cylindrical part of the terminal shell [11]. The two CPO are positioned 180 degrees apart. In some cases, currents of the resistor chains, installed on both the acceleration and deceleration tubes and on the column's guarding rings, are used for estimating the HV value.

3.1 Generating voltmeter

In operation of the cooler's Pelletron, the main tool for measuring and stabilizing the energy is the GVM, which consists of a stator, a propeller, and a motor (Fig.3.1). Most of the time, the so-called 4" GVM was used. The GVM's stator has 8 electrically connected, isolated from ground sensor plates placed between grounded plates of the same size. In front of them, an 8-blade, 95 mm-diameter propeller rotates at 60 Hz chopping the electric field produced by the terminal voltage at the sensor plates. It creates a rectangular-shaped in time, 480 Hz current that is amplified and rectified in the GVM preamplifier. The resulting signal is sent to the Terminal Potential Stabilizer

(TPS), where it is used for HV regulation, and to a CAMAC for digitizing. The upper frequency for the GVM signal in the TPS is ~10 Hz.

In October 2008, the 4" GVM failed and was replaced by a more standard, so-called 2" GVM. It has the same main features but smaller diameter and 4 blades instead of 8. While no measurable changes have been found in operation, it is useful to note that all measurements described in this paper have been made with the 4" GVM.

3.2 Capacitive pickups (CPO)

The idea behind placing two CPO into the Pelletron is to use their sum signal in the regulation to suppress the HV ripple while eliminating effects of the mechanical motion of the terminal shell with respect to the tank. However, in the preliminary tests, we were not able to find modes where using the CPOs would be beneficial [12]. In normal operation the CPO gain is set to zero so that the CPO signals are used only for diagnostics and protection purposes. In addition to NEC-provided electronics, two types of amplifiers were attached to one of the CPOs. One of them is sensitive in the bandwidth of 100 kHz - 10 MHz and is used for recording the fast changes of the HV. In addition, the signal feeds the electronics that close the electron gun in about 1 μs if the terminal voltage quickly drops by more than 5 kV in order to prevent full discharges [13]. The second additional CPO amplifier has a bandwidth of 0.1 – 100 Hz and is used to observe the voltage ripple and jumps, first of all, when the GVM is suspected to be malfunctioning.

Figure 3.1 Photo of the 4" GVM installed in the Pelletron tank.

3.3 Beam-based energy diagnostics

The beam trajectory is measured by 31 pairs of capacitive pickups, referred to further as beam position monitors, or BPMs [14]. For the BPMs to detect the position of the DC electron beam, a low-amplitude sinusoidal 32 kHz modulation is applied to the beam current. In the so-called "slow" processing mode, the control system receives the BPM signals at 1 Hz with a typical level of the electronics-generated noise below 10 μm. All BMP positions are continuously data logged at 1 Hz, which allows offline analyses of the trajectories.

Dispersion in the electron beam line is suppressed up to the end of the cooling section down to < 10 cm but increases up to several meters further downstream (Fig. 3.2).

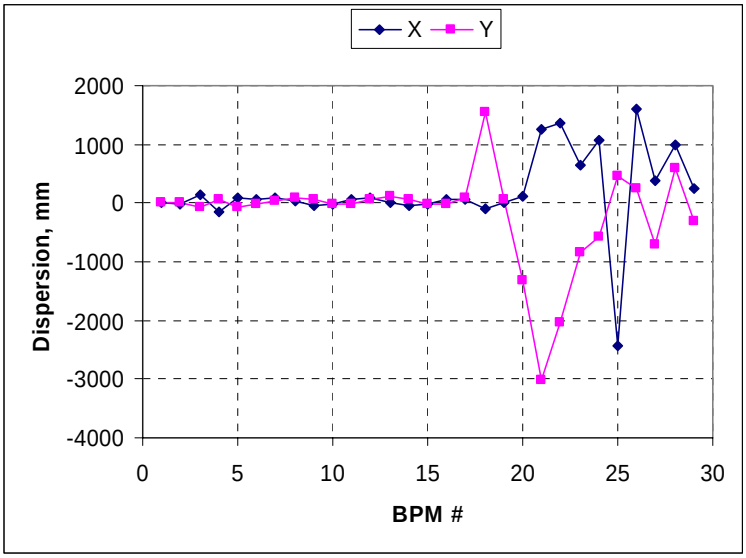

Figure 3.2. Dispersion in the electron beam line. Dispersion is measured from the differences Δx, Δy between BPM readings at two Pelletron voltages and expressed as $\Psi_x = \Delta x / \left(\frac{\Delta p}{p} \right)$, $\Psi_y = \Delta y / \left(\frac{\Delta p}{p} \right)$, where p is the average electron momentum and Δp is the difference between momenta at these voltages. The horizontal axis shows the BPM number counted along the beam line. The first BPM after the cooling section and 180 deg bend, called R01, is #18 on the plot. Reading of its vertical channel, called BYR01, varies with energy changes at the rate of 0.33 mm/keV.

The momentum aperture of the cooler allows stable beam recirculation with changes of the electron energy by up to at least +/-5 keV, well above the level harmful for the cooling strength. Therefore, changes of the beam position in the high-dispersion BPMs can be used to calculate corresponding changes of the beam energy in the interesting range. However, whether this diagnostics is useful depends on its noise and stability.

Part of the noise comes from BPM electronics; some other part comes from the trajectory jitter caused by Pelletron vibrations etc, but the largest contribution is

caused by the Main Injector (MI), a 150-GeV synchrotron with which the Recycler ring shares the tunnel. The magnetic field of MI's current busses and magnets significantly (by several millimeters) moves the electron beam in the return line. To separate the various sources of noise, we first verified that readings of high-dispersion region BPMs can provide information about the energy when the MI is not ramping.

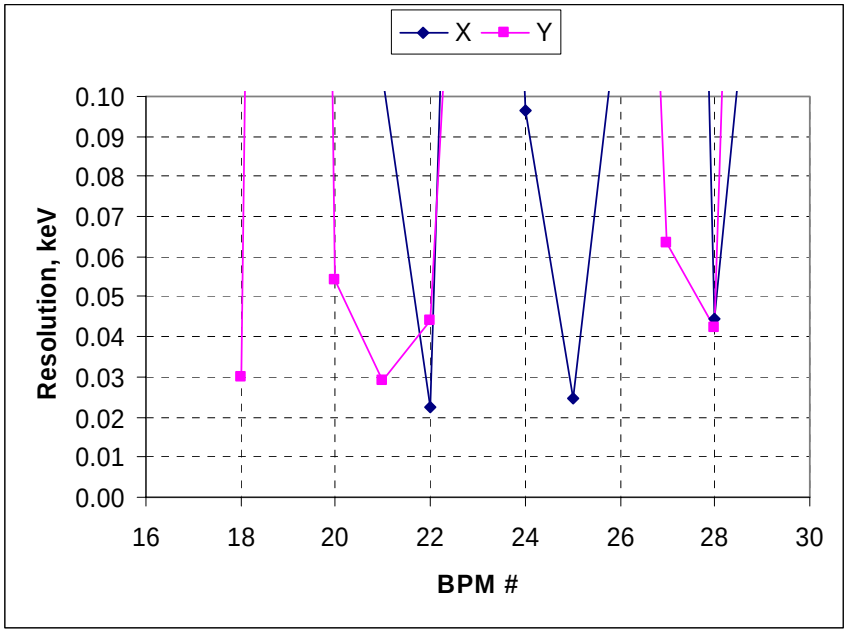

Figure 3.3 Energy resolution for various BPM channels. The resolution was calculated from measurements used in Fig.3.2 as $\Delta E \cdot \left(\frac{\delta X}{\Delta X} \right)$, where ΔE = 4.8 keV is the difference in energy between two measurements, ΔX is the difference between averaged readings of the beam position in a BPM channel, and δX is the rms error of this difference caused by the noise of electronics and beam motion. BPM readings with 0.1 Hz filtering were used. The best resolution is at BYR01 (#18 on the plot), BYR04 (#21), BXR05 (#22), and BXT03 (#25).

In part, we analyzed 13 hours of 1 Hz data recorded on April 12, 2008 for constant settings of the cooler beam line and with no ramp in the Main Injector. Readings of four BPMs in the return line (Y- channels numbered 18, 20, 21, and 22 in Fig.3.2) were transformed into energy deviations using the dispersion coefficients from the data presented in Fig. 3.2. Correlation coefficients between the resulting four sets of data were found to range from 0.961 to 0.997, and calculated energy deviations were close for all BPMs. Therefore, in principle any of these channels (and several others, see Fig.3.3) can be used for reconstructing the energy. On the other hand, GVM readings recorded at the same time show very low correlation with these energy-related beam position deviations (outside infrequent energy jumps mentioned in the section 5.3.5). Namely, the correlation coefficient for the entire 13 hours sample was found to be 0.05. We interpret this result as a proof that in the mode without Pelletron voltage jumps, the GVM signal reported to the data acquisition system is

dominated by ADC noise with rms of 0.2 kV. Note that the HV regulation circuitry uses an analog signal, which is not affected by that noise.

In addition to the noise, this type of energy measurement can be affected by mechanical drifts of focusing elements and drifts of their power supplies. As a result, for long-term stability (days), the beam position recorded as close as possible of the 180 deg bend is preferable. In routine operation, the energy reconstruction is based on readings of the BPM which is immediately after the 180 deg bend (BYR01). A parameter calculated with a BPM further downstream, BXT03, gives a good indication of energy deviations on the scale of several hours, but significantly (~keV) drifts away in a matter of a day.

Because the electron cooling strength is regulated by a parallel shift of the electron beam in the cooling section [5], BYR01 readings vary even when the energy is constant. In operation, we use a dedicated energy deviation parameter, which is calculated, in addition to BYR01, with BPM readings in the cooling section and is expressed in keV. Moreover, BPM readings are used with 0.1 Hz filtering. Still, the optimum value of the energy parameter is drifting on a week scale and needs to be adjusted according to dedicated measurements of the cooling strength. Recently, this drift was found to be related to the 180-degree bend magnet temperature that likely changes its field strength. We plan to take this effect into account in the calculation of the energy parameter.

4. ENERGY REGULATION

The electron energy is stabilized at several levels. The main component is the standard Pelletron system based on adjustments of the corona needles current; the second is a software loop that makes GVM readings equal to the value set for the terminal voltage by changing the chain current; and finally, the set point is tuned according to the beam-based energy deviation parameter.

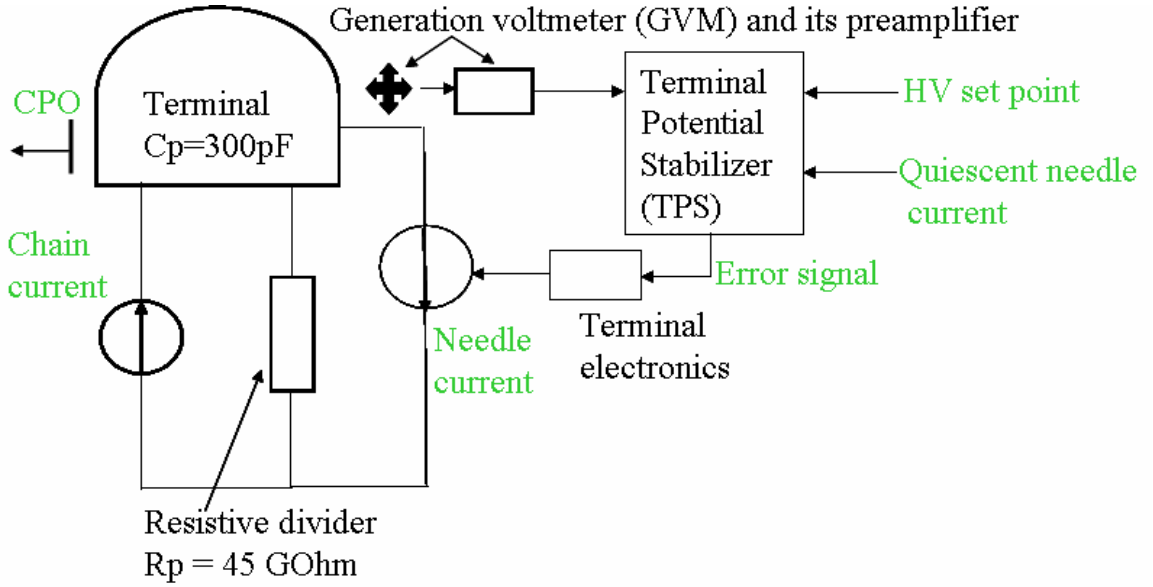

Figure 4.1. Pictorial view of the Pelletron energy regulation system.

The Pelletron high voltage (HV) regulation system [11, 15] consists of: the GVM and two CPOs with their amplifiers; the Terminal Potential Stabilizer box (TPS) where the GVM and CPOs signals are compared with the set value and an error signal is generated; fiber optics delivering the error signal to the Pelletron terminal; the terminal electronics regulating the current from the corona needles through a triode; and the corona needles themselves. A pictorial view of the system is presented in Fig. 4.1.

The performance of the system can be characterized by its response to a slowly increasing chain current while other parameters are kept fixed (Fig. 4.2).

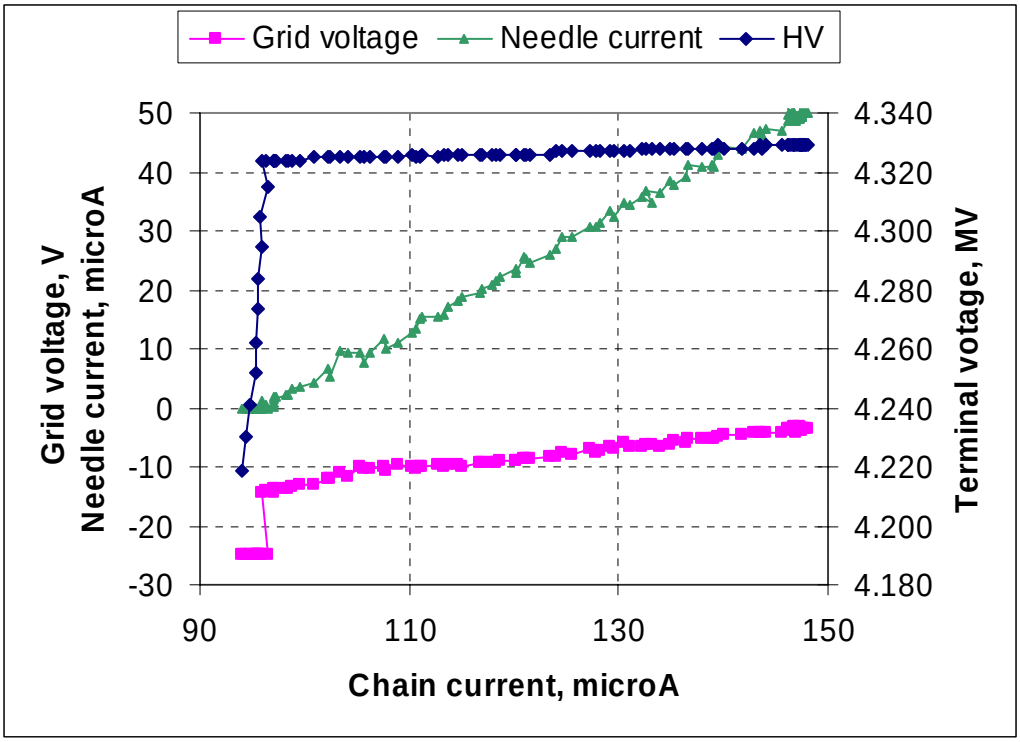

Figure 4.2. Performance of the Pelletron HV regulation system (21-Aug-08). The HV set point is 4.325 MV; the gains are set to 90% total and 0% CPO; and the quiescent current value is 15 μA. The electron beam is off. The slope of the part with HV regulation is 0.10 GOhm.

In stable conditions (i.e. negligible corona currents) and with the electron beam off (i.e. zero beam loss), the chain current I_{ch} is equal to the sum of the current through the resistive dividers and the corona needle current I_n:

$$I_{ch} = \frac{U_p}{R_p} + I_n, \tag{4.1}$$

where U_p is the Pelletron terminal voltage and R_p = 45 GOhm is the sum resistance of all Pelletron's resistor chains. At a low chain current, the regulation circuitry suppresses emission from the needle, and the terminal voltage is equal to the product $I_{ch} \cdot R_p$. When the high voltage (noted HV on the plot) approaches the set point, the

regulation system decreases the value of the negative grid voltage at the regulation triode so that the current emitted from the needles is removing the extra charge brought by the chain and the terminal voltage becomes nearly constant.

In this state, the current emitted from the needles is linear with the error signal:

$$I_n = I_{n0} + \frac{G}{R_{eff}}\left(U_p - U_o\right), \tag{4.2}$$

where I_{n0} is the so-called quiescent current, a current emitted from the needles when the terminal voltage is equal to the set value, U_o; G is the gain that can be changed from the control system from 0 to 1, and R_{eff} is the value characterizing the system. The voltage is equal to the set value only at a specific chain current I_{ch}^{*},

$$I_{ch}^{*} = \frac{U_0}{R_p} + I_{n0}\,. \tag{4.3}$$

Otherwise, it deviates linearly with the chain current:

$$U_p - U_o = \frac{R_p}{1 + \dfrac{R_p \cdot G}{R_{eff}}} \cdot \left(I_{ch} - I_{ch}^{*}\right). \tag{4.4}$$

If, in addition, there is a lost current δI either from the circulating electron beam or a corona current from the terminal, it is subtracted in Eq. (4.4) as follows

$$U_p - U_o = \frac{R_p}{1 + \dfrac{R_p \cdot G}{R_{eff}}} \cdot \left(I_{ch} - I_{ch}^{*} - \delta I\right). \tag{4.5}$$

From Eq. (4.4) follows that the inverse derivative $(dU_p/dI_{ch})^{-1}$ is linear with the gain,

$$\left(\frac{dU_p}{dI_{ch}}\right)^{-1} = \frac{1}{R_p} + \frac{G}{R_{eff}}\,. \tag{4.6}$$

Results from measuring the derivatives for different gains are shown in Fig. 4.3. The found value of R_{eff} is 86 MOhm (<< R_p = 45 GOhm).

Normally, the Pelletron is operated at G = 0.9 and I_{n0} = 15 μA. In accordance with Eq. (4.5), a drift of the chain current or current losses by 10 μA results in a deviation of the Pelletron voltage by ~1 kV. Because such events do occur (see, for example, [16]), a dedicated software loop was implemented [12]. This program calculates what changes of the chain current are needed to achieve $U_p = U_o$ and adjusts the chain current by a portion of this value. Normally, this portion is 0.5, and changes are made

every 10 seconds. Note that a similar program had been provided by NEC as well, and attempts to use it were made during the R&D phase of the project. These attempts were unsuccessful partly because of problems of communication between NEC's and Fermilab's control systems and partly because at that stage a precise HV regulation was not considered a main issue.

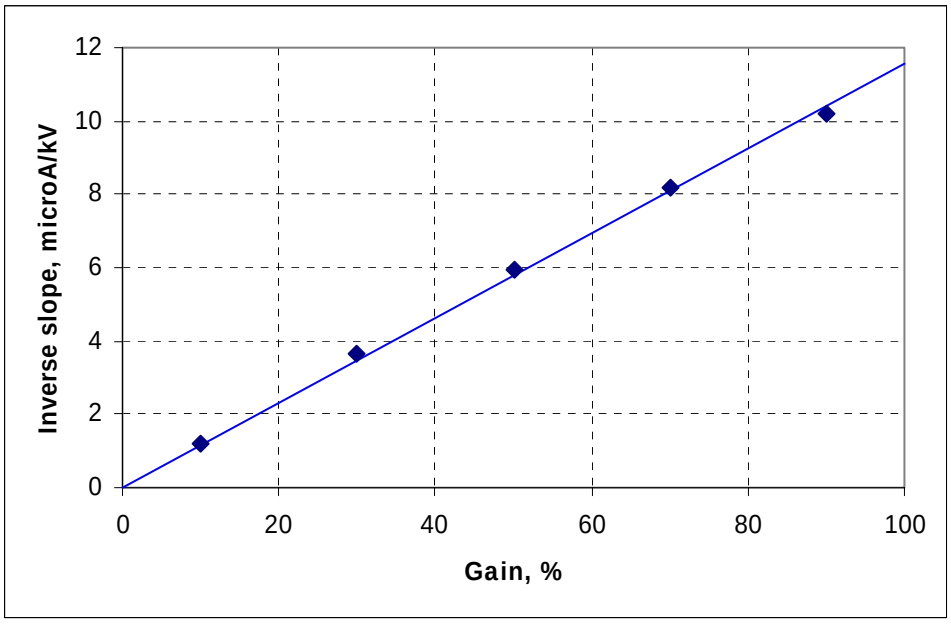

Figure 4.3. Inverse slope of curves similar to those shown in Fig. 4.2 as a function of the system gain. The solid curve is the best linear fit according to Eq. (4.6) with R_p = 45 GOhm.

If the temperature of the Pelletron or HV-regulation electronics changes significantly (see Section 5.3), the GVM reading doesn't provide the adequate value for the electron energy. To correct this deficiency, another software loop [17] reads the energy deviation parameter (see Section 3.3) and adjusts the HV set point correspondingly.

5. Electron energy calibration and stability

The Recycler is a permanent-magnet based storage ring with a fixed energy of antiprotons. Therefore, for optimum performance the electron energy needs to be constant as well, and deviations of the energy from the optimum value by more than 500 V affect significantly the cooling efficiency. One of the effects is illustrated in Figure 5.1, which compares momentum distributions of antiprotons after cooling at the optimum energy and with the electron energy shifted from optimum by 1.2 keV. For antiprotons kept between rectangular RF buckets, such a shift leads to flattening the momentum distribution.

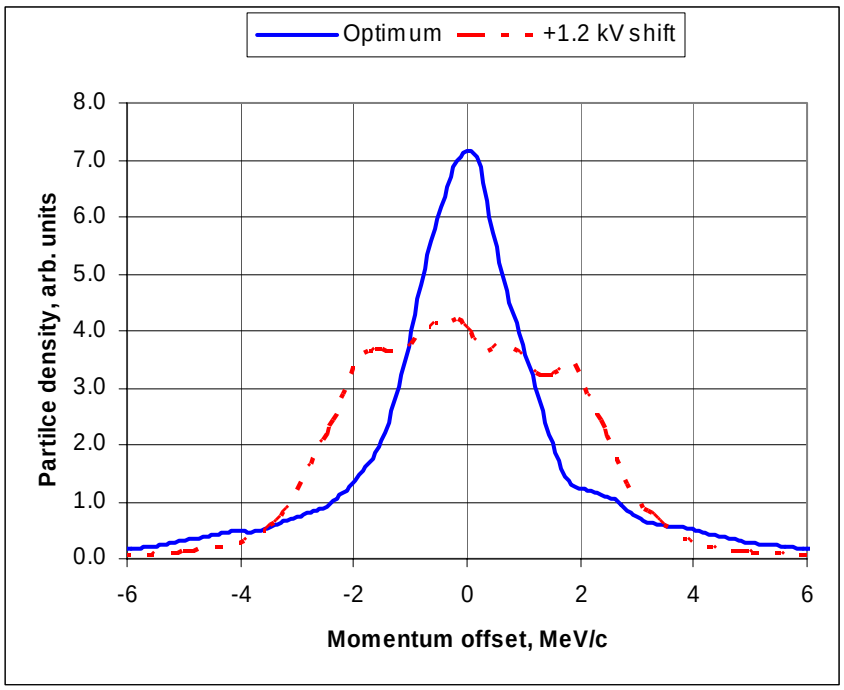

Figure 5.1. Momentum distribution of the antiproton beam electron cooled at two different electron energies. The solid blue line shows data for optimum energy tuning, and the dash-dot red line represents data for cooling with the electron energy shifted by 1.2 keV. September 10, 2008. Number of antiproton 105E10, bucket length 5.8 μs; electron beam is on axis. Vertical scale is linear.

In this chapter we describe the absolute electron energy calibration and the energy stability when all parts perform correctly. The energy stability is analyzed separately at frequencies above ~0.2 Hz ('ripple') and below 0.2 Hz ('drift').

5.1 Absolute energy calibration

After assembling the Pelletron, the GVM calibration was verified with a 100 kV external power supply and a calibrated resistive divider. The next step for calibrating the electron energy was to measure the length of a Larmor spiral pitch in the cooling section [18] at the energy close to the nominal. The resulting change of the GVM calibration was 5.2%. The precision of this measurement, determined by the calibration of the Hall probe used for the longitudinal field measurements and by the beam position measurement errors, was estimated to be ±0.2%. Final adjustments were made based on electron cooling effects. In equilibrium, an electron-cooled coasting antiproton beam has exactly the same average velocity as the electron beam in the cooling section. In turn, it allows calibrating the absolute value of the electron energy down to the precision of the Recycler energy calibration, 0.1% [19].

5.2 Electron energy ripple

Energy deviations at frequencies above 1 Hz, referred here as ripples, were analyzed by recording HV signals with the CPO and the beam trajectory with BPMs. Figure 5.2 shows the energy deviation as a function of time calculated from the CPO

and from a high-dispersion region BPM signals. FFT components of these signals are presented in Fig.5.3.

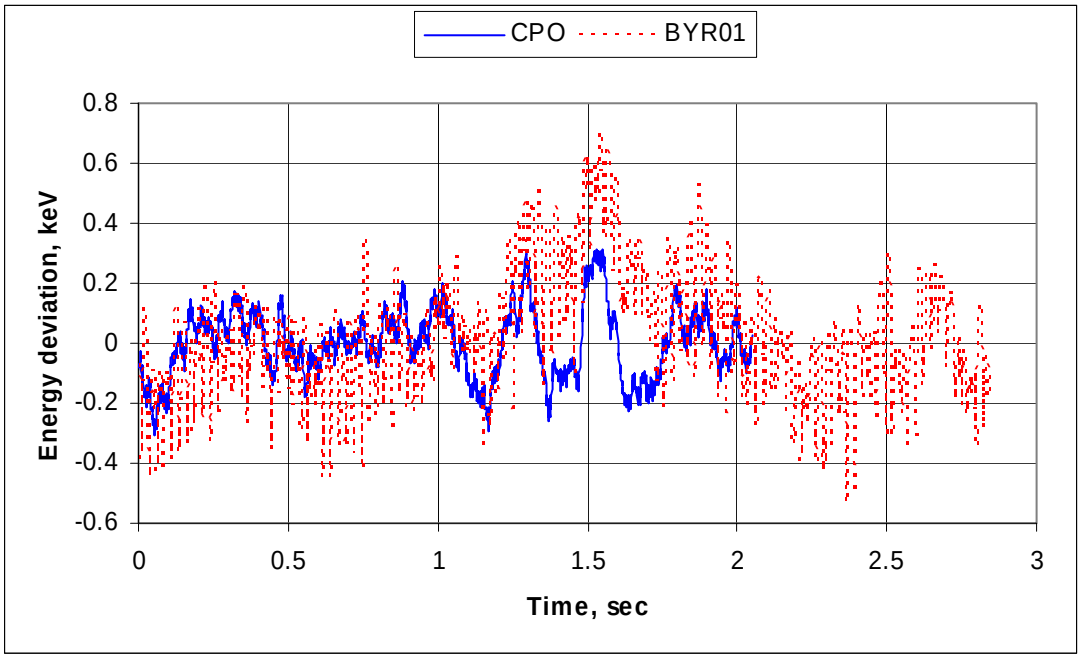

Figure 5.2. Energy deviation reconstructed from the CPO and a high-dispersion region BPM (BYR01) on May 5, 2008. 2047 points are recorded at 1 ms intervals for the CPO and 1.4 ms intervals for the BPM. The system gain was 50%, and the CPO gain was set to zero.

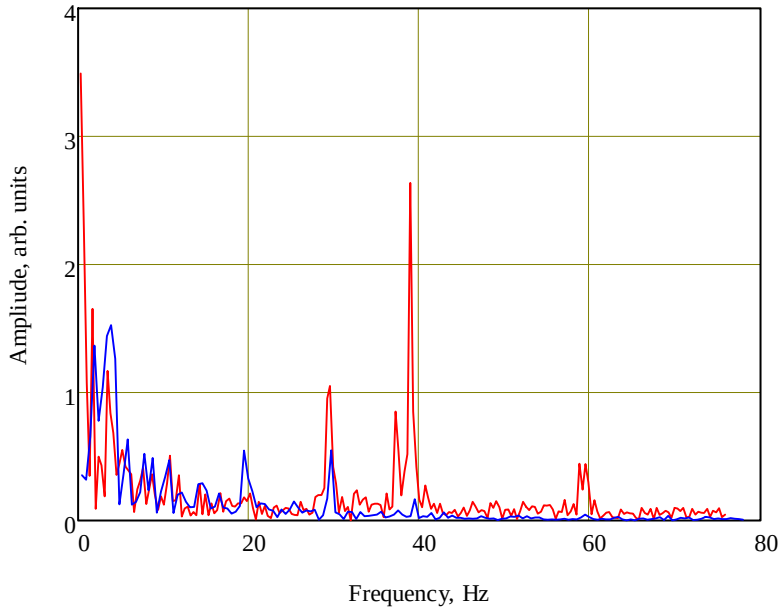

Figure 5.3. Spectra of signals plotted in Fig.5.2. Red – BPM, blue – CPO. The amplitude of the components above 60 Hz is at the noise level.

These calculations assume that both signals are generated only by the ripple of the terminal high voltage, while the analysis of the data from the cooler prototype [7] has shown that mechanical vibrations of the terminal significantly affect CPO readings and that the beam trajectory is also perturbed by these vibrations and by variations in time of stray magnetic fields as well. Results of attempts to separate voltage ripple from vibration effects using two CPOs [12] were not conclusive, and the latest analysis concentrated on using BPMs. The beam position was simultaneously recorded in all BPMs [20] at a 700 Hz sampling rate. Propagation of all frequency components through the beam line was analyzed by A. Burov using a linear optics model of the beam line. The analysis [21] showed that the high-frequency components of the BYR01 signal are explained by the beam motion upstream of the 180-degree bend, and only signals in the 1- 6 Hz range are caused almost entirely by the energy ripple. The estimated rms value of the ripple is about 150 eV.

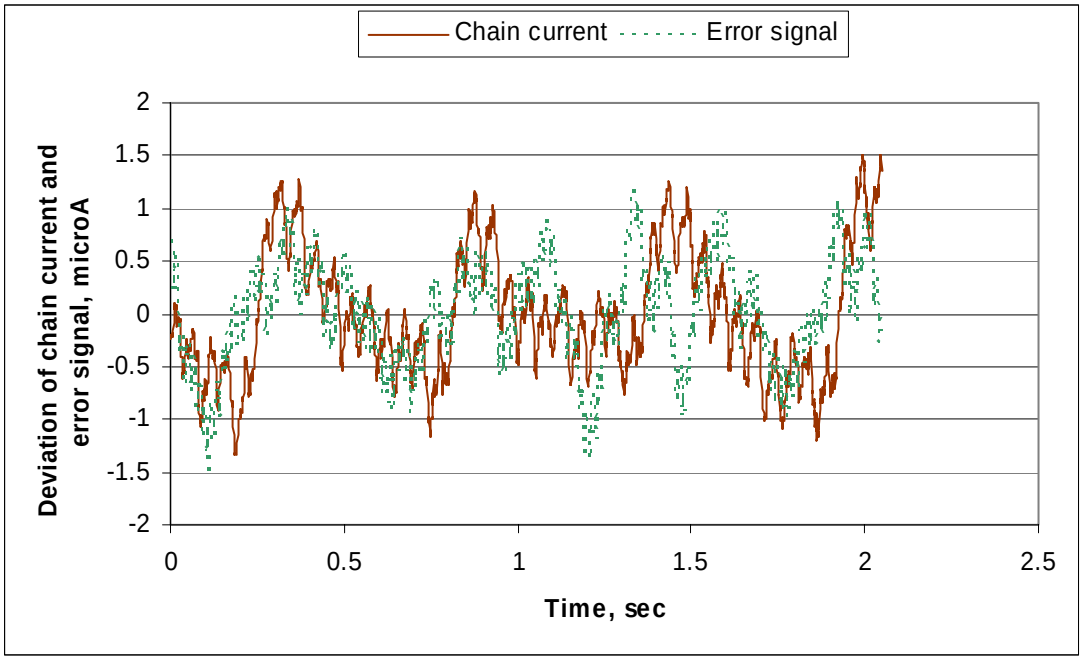

Figure 5.4. Deviation of the chain current (solid brown line) and error signal (dotted green line) as a function of time. The data were recorded simultaneously with those presented in Fig.5.2. The average values were 106.5 μA for the chain current and 14.8 μA for the error signal.

While the ripple is well within the requirements for effective cooling, it is interesting to look for its main sources. One of the additional diagnostics tools available is a the error signal generated by the TPS electronics from comparing the GVM reading with its setting, taking into the account the specified gain and quiescent current values. The error value is expressed in μA of corona needles current that the circuitry at the terminal should generate when it receives the signal through the fiber link. The error signal was recorded at a 1 kHz sampling rate simultaneously to taking the data shown in Fig. 5.2 and the AC component of the chain current (Fig. 5.4). The spectrum of the chain current almost uniquely consists of the rotation frequencies of

the chain and the chain motor (1.8 Hz and 19 Hz, respectively) and their harmonics. If the chain current ripple was the only source of energy fluctuations and the regulation circuitry bandwidth was infinite, the error signal would exactly follow the chain current changes. The difference between AC components of these currents, δI_{ch_err}, drives the voltage ripple. The spectrum of δI_{ch_err} shows that the regulation system at its present settings decreases by a factor of 3 the 1.8 Hz component, amplifies by a factor of 2 the 3.6 Hz component, does not affect higher chain current harmonics, and adds ripple at 12 and 60 Hz.

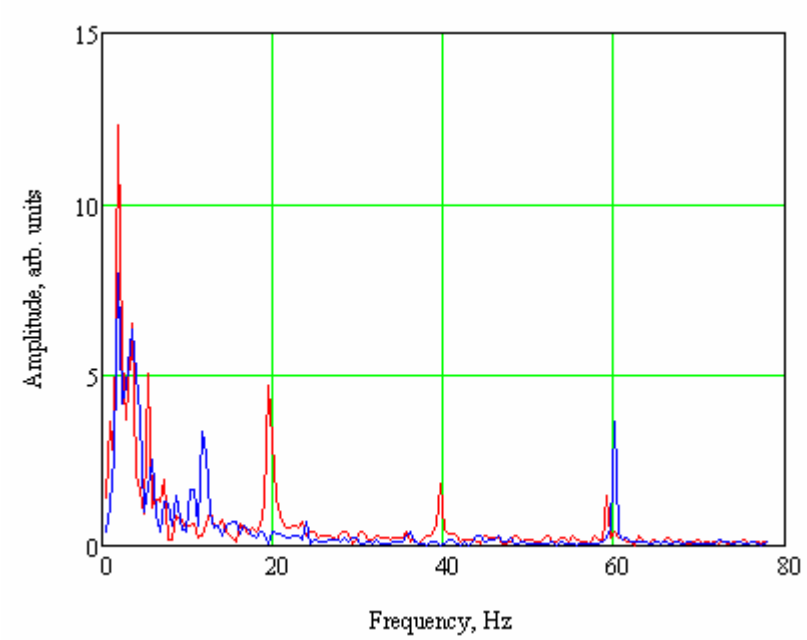

Figure 5.5. Spectra of the signals plotted on Fig.5.4. Red – chain current, blue – error signal. The amplitude of the components above 60 Hz is at the noise level.

The voltage ripple δU_{ch_err} generated by the current δI_{ch_err} can be calculated as follows:

$$\delta U_{ch\_err}(t) = \int_0^t \frac{\delta I_{ch\_err}(t_1)}{C_p} \cdot e^{-\frac{t-t_1}{R_p C_p}} dt_1 . \qquad (5.1)$$

where C_p and R_p are defined in Fig. 4.1.

In Fig. 5.6, the low-frequency spectrum of the energy deviation reconstructed from the BYR01 signal of Fig. 5.3 is compared to calculations made with Eq. (5.1) fed with the data plotted on Fig. 5.4. The closeness of the two spectra shows that the main portion of energy fluctuations above 1 Hz is, indeed, related to the chain current fluctuations and the specifics of the HV regulation system. Note that higher-frequency components are suppressed by the large value of R_pC_p = 13 sec.

To estimate the voltage ripple components at lower frequency, the BYR01 signal was also recorded at a 102 Hz sampling rate for 20 seconds. Because this measurement was made during regular operation, the beam motion caused by the Main

Injector ramping every 2.2 sec creates additional peaks at 0.45 Hz and its harmonics, 0.9 and 1.35 Hz (Fig.5.7). For comparison, a spectrum of a signal from a BPM in the low-dispersion region is shown as well. In the range down to 0.2 Hz, the data do not show any additional peaks that can be interpreted as energy ripple – related. The RMS value of the energy ripple calculated in the frequency band 1.5- 6 Hz is 90 eV. Note that this value depends on the chain current ripple and the HV regulation system gain.

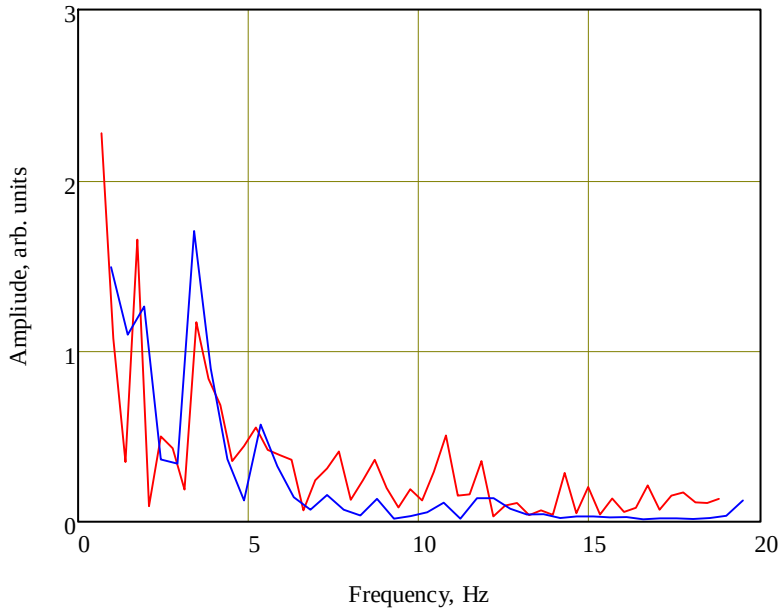

Figure 5.6. Comparison of energy spectra calculated from the BPM (same as in Fig.5.3, red) and from data shown in Fig. 5.4 using Eq. (5.1) (blue).

We did not find any measurable effect of possible fluctuating corona currents emitted from the terminal shell. The analysis of the electron beam trajectory fluctuations mentioned above [21] showed no signals above 6 Hz that can be interpreted as an energy ripple. If such a high-frequency ripple exists, it is below tens of eV rms. This conclusion agrees with the observed low corona current. One can judge about its value by looking at the so-called lost current, which is calculated as the difference between the measured values of the chain current and the sum of the resistive dividers' and needle currents. Typically, the beam loss is small (~1.5 μA) and constant, and the lost current fluctuates either as a result of terminal voltage fluctuations, when a current comes in and out of the terminal-to-tank capacitance, or when a corona current is being emitted from the terminal shell. For example, a high lost current is always observed during initial conditioning of the accelerator structure after accessing the Pelletron tank, and sometimes (~ once in a month), it jumps up and remains for seconds or even minutes (see Section 5.3.4). Outside of these events, the lost current fluctuates within 2 μA. For estimation of the worst scenario, one can assume a sinusoidal corona current with the amplitude δI_{cor} = 1 μA and a frequency right out of the reach of the regulation loop, f = 10 Hz. From Eq.5.1, the amplitude of the voltage perturbation δU_{cor} is

$$\frac{\delta U_{cor}}{U_P} \approx \frac{\delta I_{cor}}{I_{ch} - I_n} \cdot \frac{1}{2\pi f\, R_P C_p}, \qquad (5.2)$$

and numerically Eq.(5.2) estimates the ripple to be ~ 50 V.

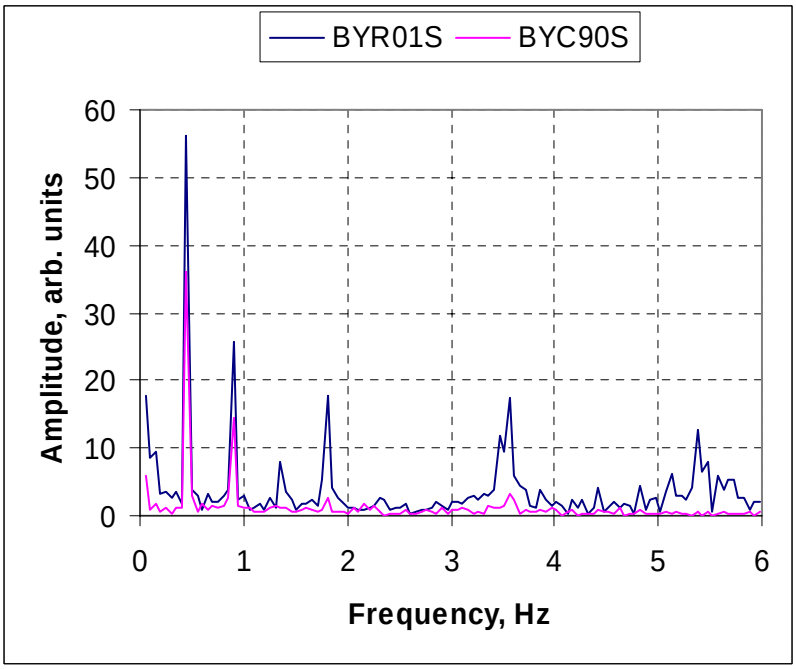

Figure 5.7. Spectra of two vertical BPMs denoted as #18 (R01, blue trace) and #16 (C90, magenta trace) in Fig. 3.2. September 15, 2008. 2047 points were recorded for each BPM at a 102 Hz sampling rate. Components below 1 Hz are caused by beam motion induced by Main Injector ramps with 2.2 sec period. The RMS value of the energy ripple calculated in the frequency band 1.5- 6 Hz is 90 eV. The system gain was 90%, and the CPO gain was set to zero.

5.3 Electron energy drifts

The electron energy was changing significantly over periods ranging from tens of seconds to days, forcing adjustments of the set point for the high voltage using beam-based measurements. Over the years of operation, several causes of the drift were recognized and corrected or taken into account.

5.3.1 Drift caused by the tank temperature deviation

The most obvious effect was the drift related to the changing temperature of the Pelletron tank when starting the machine, illustrated in Fig.5.8. The measured energy change with respect to the change of the temperature of SF6 exiting the tank is ~ -0.4 keV/K. If one assumes that the effect is caused by an axially symmetric thermal expansion of the steel tank and aluminum terminal shell, the coefficient should be an order of magnitude lower, -0.03 keV/K. Part of this discrepancy can be related to significant temperature gradients in the tank. When the Pelletron is far from equilibrium, the assumption that the temperature of all elements inside the tank is equal to the temperature of the SF6 exiting the tank can be inadequate. However, a

more likely explanation is that the entire column tilts during temperature variations. For example, if while heating up, the column bends towards the GVM so that the 0.8-m gap between the GVM and the terminal shrinks by, let say, 0.8 mm, the feedback loop decreases the terminal voltage by 0.1% to keep the same electric field at the GVM propeller, and, therefore, decreases the energy by the same amount.

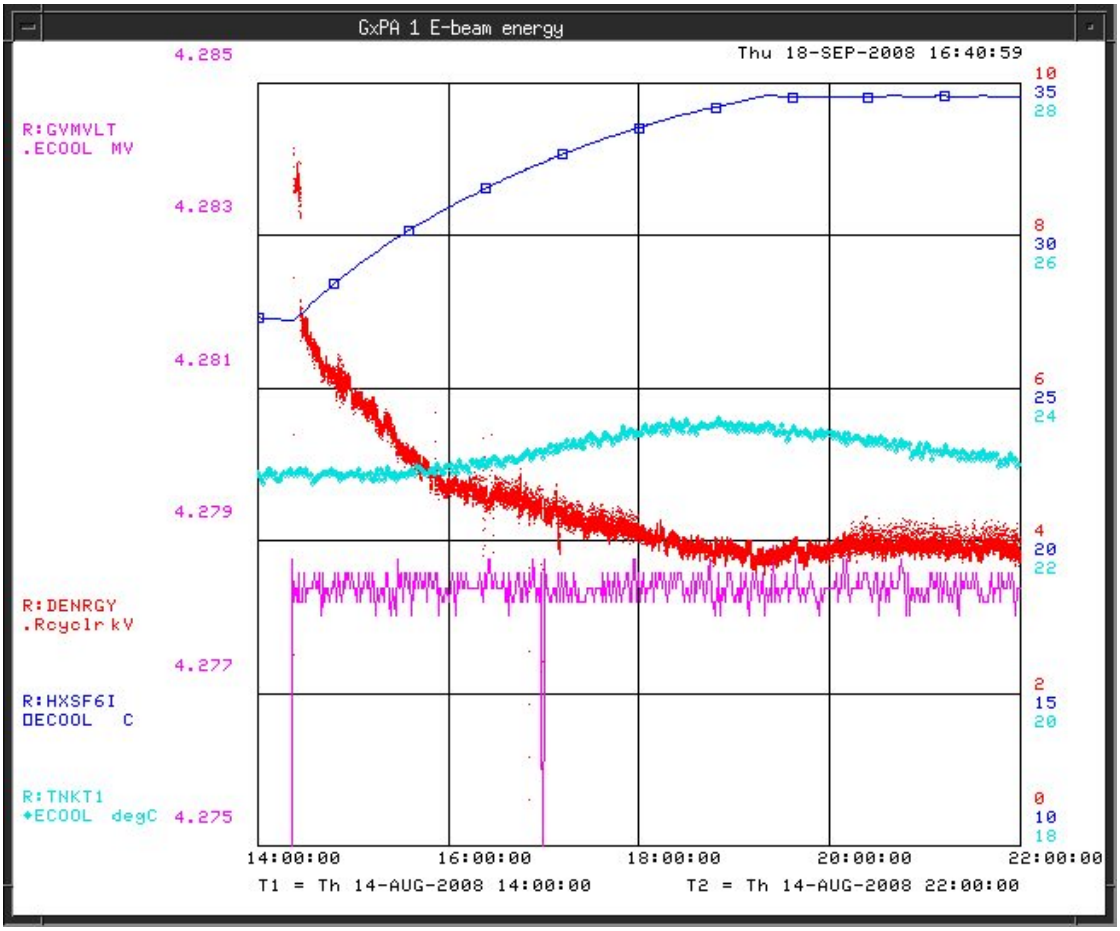

Figure 5.8. Example of the electron beam energy evolution after turning the accelerator on. The red trace shows the energy deviation parameter in keV; the dark blue trace is the temperature of the SF6 gas exiting the tank; the magenta trace shows that the HV reading by the GVM stays constant, and the cyan trace indicates the temperature of the GVM preamplifier (outside the tank).

While the exact reason for the energy deviation is unclear, the effect is quite reproducible. To alleviate it, the Pelletron is turned off only when it is necessary. In addition, when the Pelletron is being started, cooling of the SF6 gas is turned off until its temperature comes close to the final equilibrium, which decreases the time of significant temperature changes down to about 4 hours. In steady state, the SF6 cooling system keeps its temperature within ± 0.2 K [22]. Because a large portion of the heat load is removed from the Pelletron tank through the tank walls and then by the air, the ambient temperature affects the cooling efficiency of the tank and thus the

voltage stability. Presently, three air conditioning units keep the temperature in the building within ± 1K.

5.3.2 Effect of the GVM preamplifier temperature

Empirical tests showed that the most important energy drift component in a steady-state operation was related to the temperature sensitivity of the GVM preamplifier, which converts the AC component of the charge generated by the GVM propeller into a 0-10 V signal.

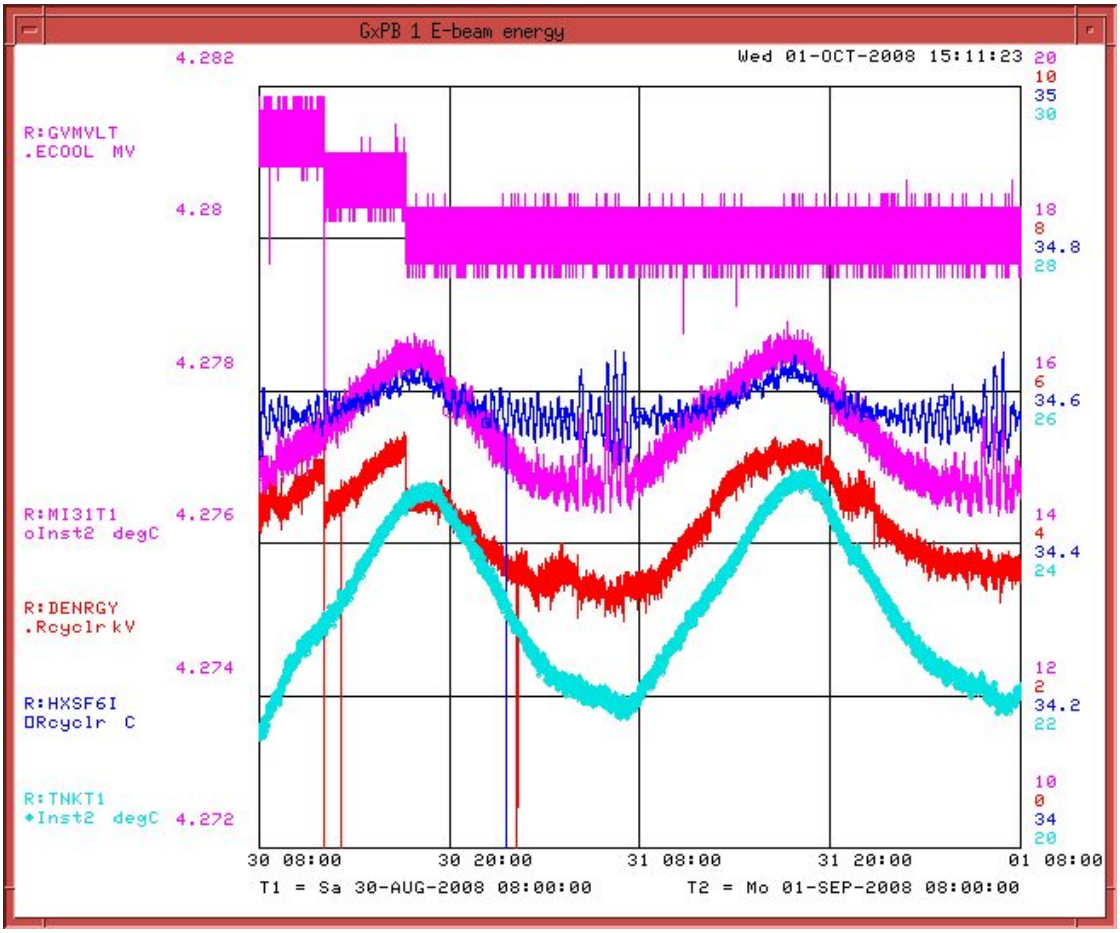

Figure 5.9. Typical energy variations over a two-day period before implementation of the thermal stabilization of the GVM preamplifier. The top magenta curve shows the GVM reading (2 kV/div). The value reported by the GVM in this plot deviates from the correct absolute calibration by 1.5% as a result of the GVM mechanics replacement in April 2008. The steps represent adjustments to keep the energy at the optimum value when the strongest cooling was required. The lower magenta curve is the air temperature in the building housing the Pelletron (2 K/div). The blue curve is the temperature of the SF6 coming out of the Pelletron tank (2 K/div). The cyan curve is the temperature of the GVM preamplifier (2 K/div).

The energy dependence on the GVM preamplifier's temperature was found to be 0.5 keV/K. Part of the problem is that the preamplifier is positioned in front of an air

conditioning unit. Between periods when the unit was blowing cold air and when it was off, the preamplifier temperature was changing by up to several Kelvin, depending on the length of the periods. When the issue was recognized, it was addressed in several ways. First, this air conditioning unit was set to be continuously on when the Pelletron tank is warm (the building temperature is still regulated by the two other units). Second, the preamplifier was put into an insulating box that smoothened out external temperature variations. Still there were temperature variations of up to ± 1.5 K with a 24 hour periodicity (Fig.5.9). Finally, a thermal regulator was added to the box, and now this temperature varies typically within ± 0.5 K over several weeks, effectively eliminating this source of the drift.

At this time, the energy drift caused by the temperature sensitivity of the other electronics is believed to be negligible.

5.3.3 GVM reading and gas permittivity

The GVM measures the charge induced by the terminal voltage at the propeller blades when they are exposed to the terminal's electric field. The amplitude of the charge variation is proportional to the total charge induced at the tank wall

$$\Delta Q \equiv C_{GVM} \cdot U_P \prec C_p \cdot U_P . \qquad (5.3)$$

When the tank is filled with SF6, the capacitance increases by the value of the SF6 permittivity ε_{SF6} (in comparison with vacuum), and, correspondingly, the value read by the GVM at the same terminal voltage increases by the same factor [23]. For normal conditions, ε_{SF6_n} = 1.0020 [24]. Assuming that (ε_{SF6} -1) changes proportionally to the gas density, at the operational pressure of ~6 atmospheres (absolute) ε_{SF6} = 1.012. Because for air at normal conditions ε_{air} = 1.00026, a GVM calibration performed in air should be adjusted by 1.2%. In operation, we observed this effect when the SF6 pressure steadily decreased over a few months due to a leak and especially when adding gas into the system. An increase of the absolute SF6 pressure by 5% results in the change of GVM reading by about 0.05% in agreement with ε_{SF6} = 1.01. The described effect is infrequent and does not cause any noticeable operational problems.

5.3.4 Energy deviations caused by misbalance of currents

As discussed in Section 4, the analog HV regulation system brings the GVM readback to the value equal to its set point only at a specific balance between the chain current and currents loading the Pelletron. A shift of this balance results in a deviation of energy from the nominal in accordance with Eq.(4.5). Numerically, a 10 μA misbalance results in a deviation of the Pelletron voltage of ~1 kV at the nominal parameters.

This effect was obvious when the charging system began to degrade, causing the chain current to decrease at a given charging voltage [16]. Implementation of the software loop that periodically adjusts the charging voltage to optimize the chain current allowed running in a wide range of charging efficiencies.

Another type of misbalance occurs when the lost current suddenly jumps by 5 - 20 μA (the lost current is calculated as the difference between the chain current and the sum of the resistive divider currents and the needle current). We interpret such events as bursts of the corona current from the terminal when a whisker appears at its

surface. If the current jump is below the value of the quiescent current (usually 15 μA), the HV regulation system is capable of stabilizing the voltage (Fig.5.10). Such events are normal after opening the Pelletron tank, and become less frequent after several days. When the lost current is higher than the quiescent current, the needle current drops to zero while the terminal voltage still decreases by tens of kilovolts or more, and the protection system turns the electron beam off. Because in steady state running these bursts happen less than once in a week and last for a minute or so, presently it is not considered as a significant problem.

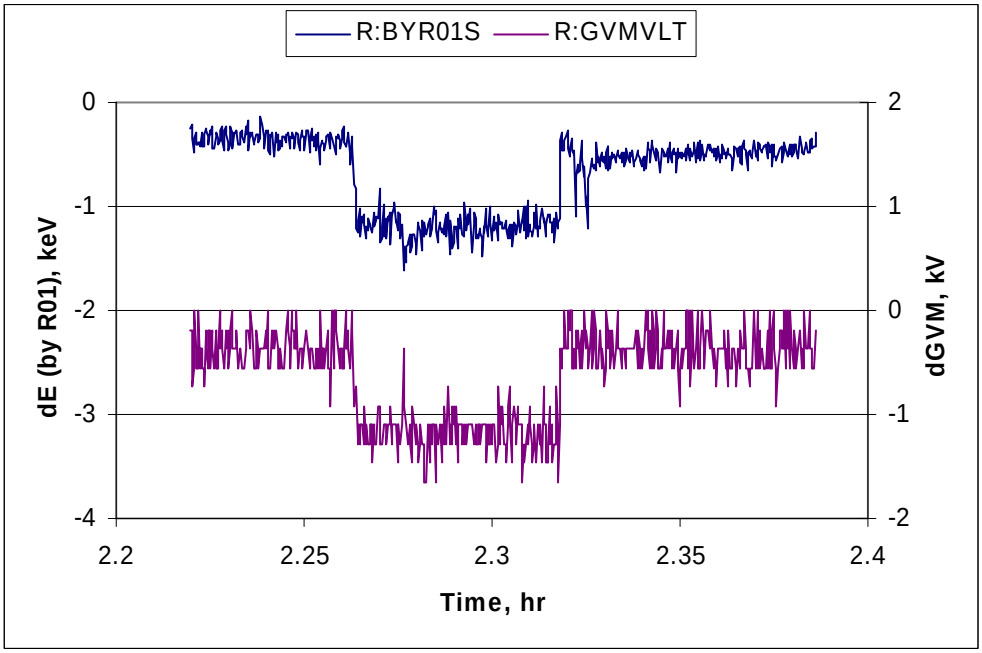

Figure 5.10. Decrease of energy caused by a jump of the lost current by 5 μA (not shown at the plot). The HV regulation system gain was G = 0.5. April 12, 2008. MI was not ramping. The software HV regulation loop was not functioning at that time.

5.3.5 Unexplained energy jumps

Sometimes, energy jumps at a constant GVM reading are observed. An example of such event is shown in Fig. 5.11, when the energy deviates from its nominal value by as much as 8 keV for a couple of seconds, while the GVM signal stays constant. Normally such events are visible only during special analyses that separate effects of trajectory shifts in the cooling section and moves caused by the MI ramps from 'real' energy deviations, because the operational energy deviation parameter uses 0.1 Hz-filtered data, which smoothes out short-duration signals.

Also, we observed longer jumps, when the energy decreases by ~1 keV over several seconds and then slowly recovers over several minutes. Such deviations were recorded both in normal operation and in the U-bend mode. An example of the latter is shown in Fig.5.12 where minutes – long decreases in electron energy are not accompanied by changes of the GVM reading.

All jumps are always down, and the only consistent interpretation is that during such jumps the GVM reports an overestimated value of the terminal voltage.

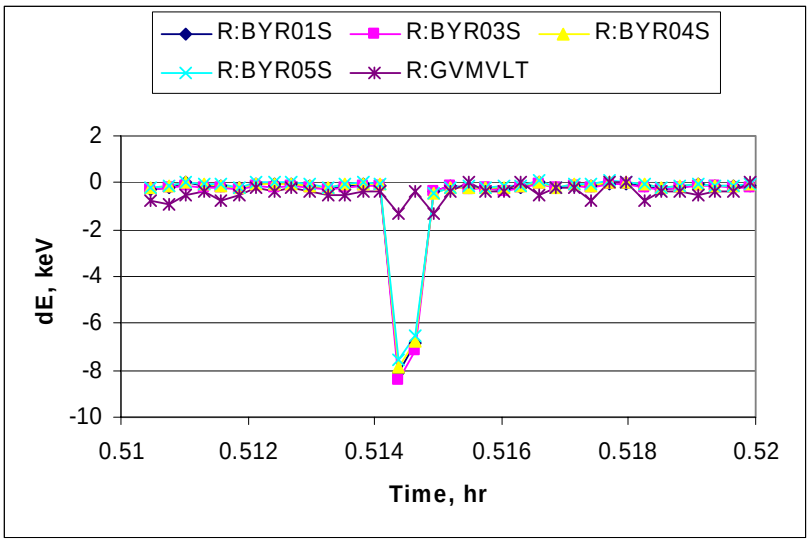

Figure 5.11. Example of an event with energy deviation at a constant value of GVM reading. All machine parameters are fixed; the MI is not ramping. Deviations of GVM readings from its average value are shown by the trace labeled R:GVMVLT. Four other traces show the energy calculated from the beam position in four corresponding BPMs. Data were recorded at 1 Hz. Data of April 12, 2008.

We do not have a convincing explanation for these jumps. First, the favorite hypothesis was the appearance of an emitting center (let say, a dust particle) at the terminal surface right opposite the GVM, so that the corona current from the center irradiates the GVM. The GVM propeller would chop the DC corona current creating a signal that would have the same temporal structure as the one produced by the terminal electric field. To estimate the order of magnitude of the emitted current that is required to explain a ~1keV energy variation, let's assume that the spot irradiated by the electrons is similar to the colored spot on the tank wall opposite to the HV regulation corona needles. The GVM propeller has about the same diameter, and to be detected, the electrons need to come to the insulated GVM plates, which account for about 45% of the surface of the spot. The electric field at nominal 4.3 MV creates at the output of the GVM a current of about 100 μA (peak-to-peak). Therefore, to explain the relative variation of energy by $2.3 \cdot 10^{-4}$, the emitted current should be ~50 nA. This value is certainly much lower than the typical noise of the lost current parameter, which would be indicative of an additional corona current, and the hypothesis seems plausible. Note that in such a process the energy jumps are always negative.

However, presently we tend to relate the jumps to an unevenness of the GVM rotation. Unstable readings of the GVM were obvious when the GVM bearing failed (see Section 6), and we speculate that the less dramatic deviations like the one on Fig. 5.11 could be caused by, let say, a dust particle reaching the bearing and then being ground out. However, the temporal structure of the energy deviation in the time of GVM failures and in the jumps under discussion is quite different; also, direct measurements of the rotational frequency did not show any noticeable perturbations.

For example, for the event presented in Fig.5.11, the frequency recorded at 1 sec intervals did not show deviations larger than 0.2 Hz.

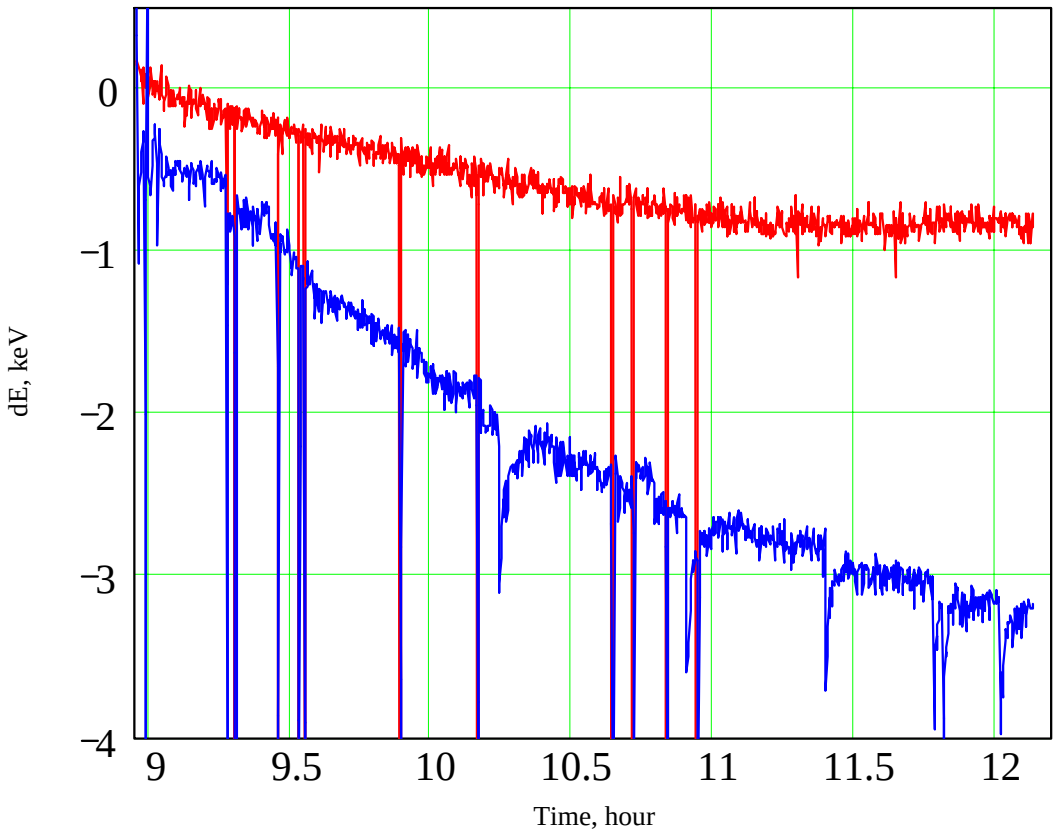

Figure 5.12. Energy jumps while working in the U-bend mode. The red curve shows changes in the GVM reading, and the blue curve is the beam energy calculated from a beam shift in a BPM located at high dispersion. The GVM signal drift is consistent with a decline of the chain current during the measurement by 6 μA. The software HV regulation loop was not functioning. The slow energy drift is consistent with changes in the tank temperature. Out-of-scale jumps correspond to recirculation interruptions. March 29, 2006.

These energy drops do not cause serious operational problems because they are infrequent and typically short. We have paid a close attention to them primarily suspecting that they are precursors of coming failures.

6. OPERATIONAL EXPERIENCE

The present HV regulation system has been used for about 8 years and in the last three years, it worked continuously most of the time (24 hours a day, 7 days a week). While it has demonstrated a remarkable reliability, there were several failures (Table 6.1).

Table 6.1. History of failures of the HV regulation system. Listed in the table are the cases when a shutdown was triggered by a HV regulation problem.

Date	Indication of the problem	Repair	Downtime to repair
27-Sep-01	Intermittent HV regulation; lost control over needle motion	Needle assembly was re-assembled	4 days
30-Apr-02	GVM motor failed	New motor installed	4 days
9-Feb-07	Intermittent HV regulation	Replaced failed PS in TPS	7 hours
18-Dec-07	Tungsten needles evaporated	Replaced by sewing needles	27 hours
19-Jan-08	Large HV noise	Cleaning and soldering connections	30 hours
10-Apr-08	Poor HV regulation	Replacement of GVM bearings	47 hours
22-Jul-08	No HV regulation	Needle current triode was replaced	25 hours
Oct-08	Increased HV noise and energy drift	Replacement of GVM bearings	During regular shutdown
28-Oct-08	Increased HV noise and energy drift	4” GVM was replaced by 2” one	24 hours

Diagnosing the failures was simple only in two cases in the first years of R&D. One of them was the correction of mechanical problems with the mechanism moving the needles assembly (so-called corona probe) and improving the electrical connections in the needles current circuitry. Another case was the replacement of the GVM motor that had burned-out coils.

After several years of problem-free operation of the HV regulation system, in February 2007 the GVM readings became intermittently unstable. Eventually, the problem was traced to the error signal, which determines the corona current to be emitted from the needles. This signal is formed in the Terminal Potential Stabilizer (TPS) and sent to the Pelletron’s terminal via a fiber optics. Normally, this signal is the sum of the set value of the quiescent current and a value proportional to the difference between the GVM reading and the HV set point. But at that time, it was changing almost randomly. Investigation found a failed internal power supply in the TPS, and normal performance returned after repairing of the supply.

In the fall of 2007, episodes of an unstable GVM readings reappeared. For periods going from minutes to an hour, the GVM reading was oscillating to up to 3 kV with typical times ranging from sub-seconds to tens of seconds. In this case, the error signal was following deviations of the GVM correctly. Additional diagnostics installed at the terminal showed that the error signal came correctly to the terminal electronics, but the triode grid voltage generated by this electronics deviated from its appropriate value. Nothing obvious was found upon opening the tank. However, when several

connections in the electronics right upstream of the triode were cleaned or soldered and the tank closed, the HV regulation began working properly.

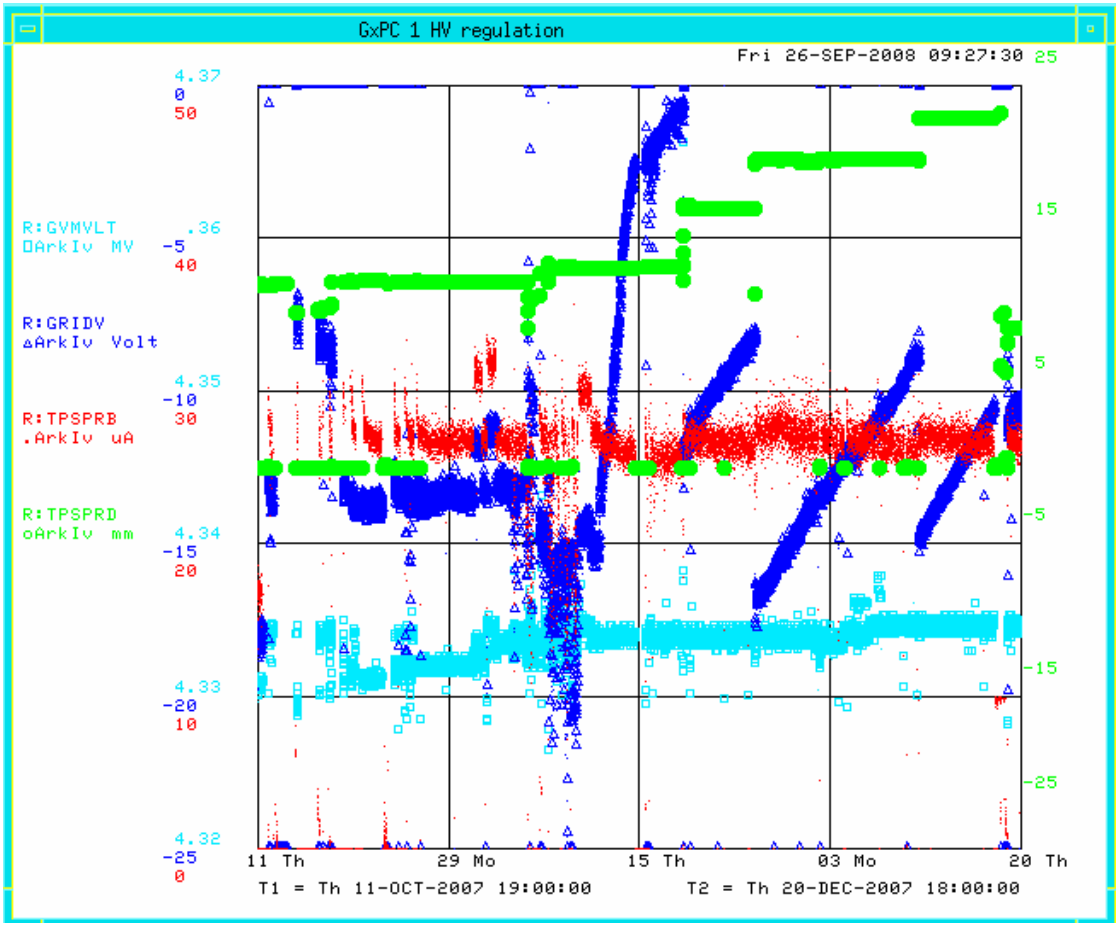

Figure 6.1. History of several parameters relevant to HV regulation over the two months preceding the replacement of tungsten corona needles on December 18, 2007. The cyan trace shows the GVM reading (10 kV/div); the dark blue trace is the grid voltage of the triode that regulates the needles current (5V/div); the red trace represents the needle current (10 μA/div); and the green trace is the position of the needles (5 mm/div). The larger value of the needles position corresponds to the needles tips being further out of the terminal shell. Data are presented at once per 5 min rate.

At the same time, the dependence of the needle current on the grid voltage of the triode dramatically shifted. Note that normally for corona needles we use regular sewing needles, replacing them once a year. Hoping to make the needles performance more stable, in the summer 2007 shutdown expensive tungsten (98.5%W, 1.5%La) needles were installed. After two months of continuous running and one week after HV instability periods appeared, the grid voltage needed to keep a given needle current started to drop. The relationship between the needle current and the grid voltage was being restored by moving the needles out more and more (Fig. 6.1). The move corresponded to the evaporation of the needles at the rate of 0.2- 1 mm per day

(with the average current from the three-needle assembly being 15 μA and around the clock operation). The diagnosis was confirmed after opening the tank, and installing again the sewing needles corrected the problem. However, we do not have any explanation why this evaporation started and why it almost coincided with the onset of instability of the HV regulation.

In spring of 2008, the energy stability degraded significantly, while the GVM reading stayed constant (only with an increased noise). In addition, abnormalities of the GVM rotation were heard if one stayed near the tank. Opening the tank confirmed that the GVM bearings had been severely damaged (Fig.6.2). Replacing the bearings restored a stable operation.

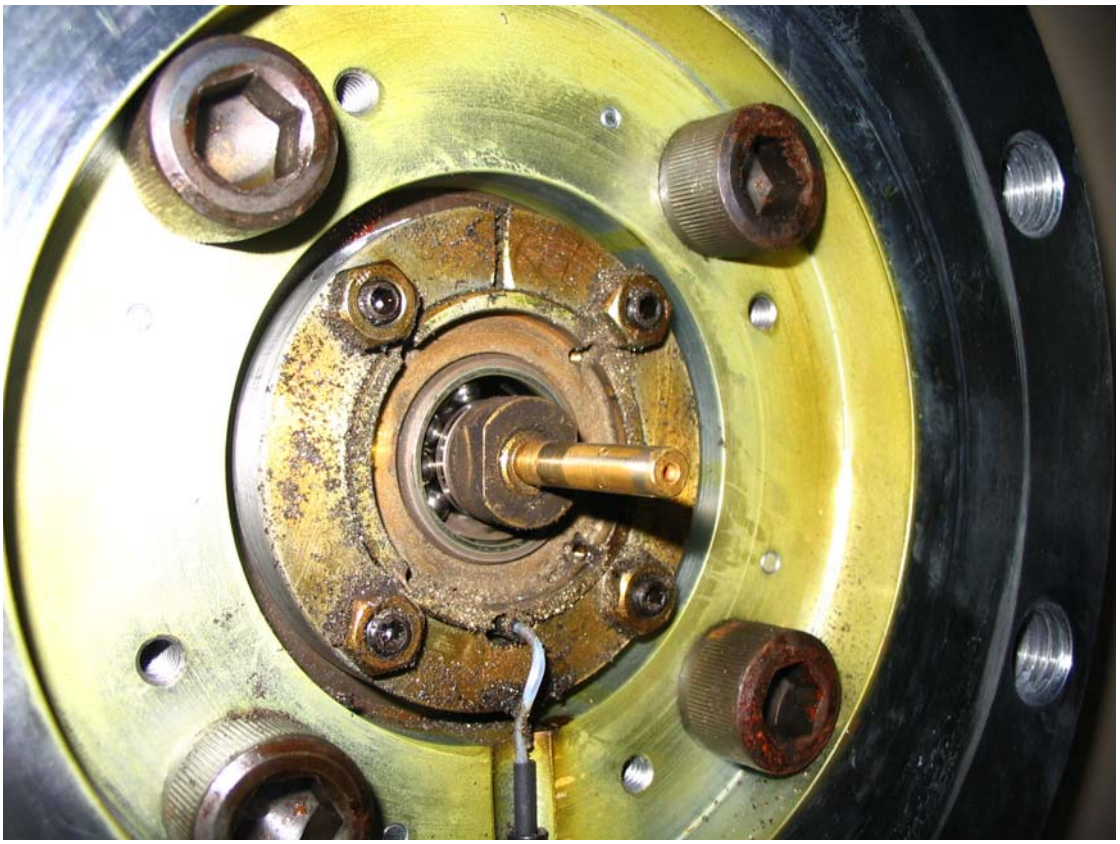

Figure 6.2. Damaged GVM bearing found in the time of the GVM repair on April 8, 2008.

The HV regulation suddenly stopped working in July 2008. This time, the GVM reported correct values and the error signal was propagating correctly all the way to the voltage of the grid of the triode. At the same time, the needle current was changing with no relation to the grid voltage. Interestingly, we were still able to provide some cooling by turning off completely the hardware HV regulation loop and speeding up the software loop that adjusts the chain current (Fig.6.3). The energy fluctuated up to 3 keV, but the average value remained constant. Replacing the triode resolved the issue.

Two more cases of HV instabilities, in September and October 2008, once more showed a disconnection between the beam energy and the HV reported by the GVM. Analysis of the signals and the replacement the GVM preamplifier convinced us that the problem was coming from the GVM mechanics. The 4" GVM was repaired during the October 2008 shutdown, but failed in a matter of two weeks and was replaced by a 2" GVM, standard for NEC.

In 2008, the failures of the HV regulation system were the one of two major reasons for the electron cooler downtime (the other one was failures of communication between Fermilab's control system, ACNET, and the Pelletron control system, ACCELNET, which accounted for ~ 10 hours per month). It is difficult to affirm whether 5 cases of HV regulation problems in one year after many years of stable operation have independent reasons (as we assume) or have something in common apart from the Pelletron age. Still, since the last shutdown in Fall 2007, the cooler ran for 92% of time (with some of the downtime not being related to the cooler problems).

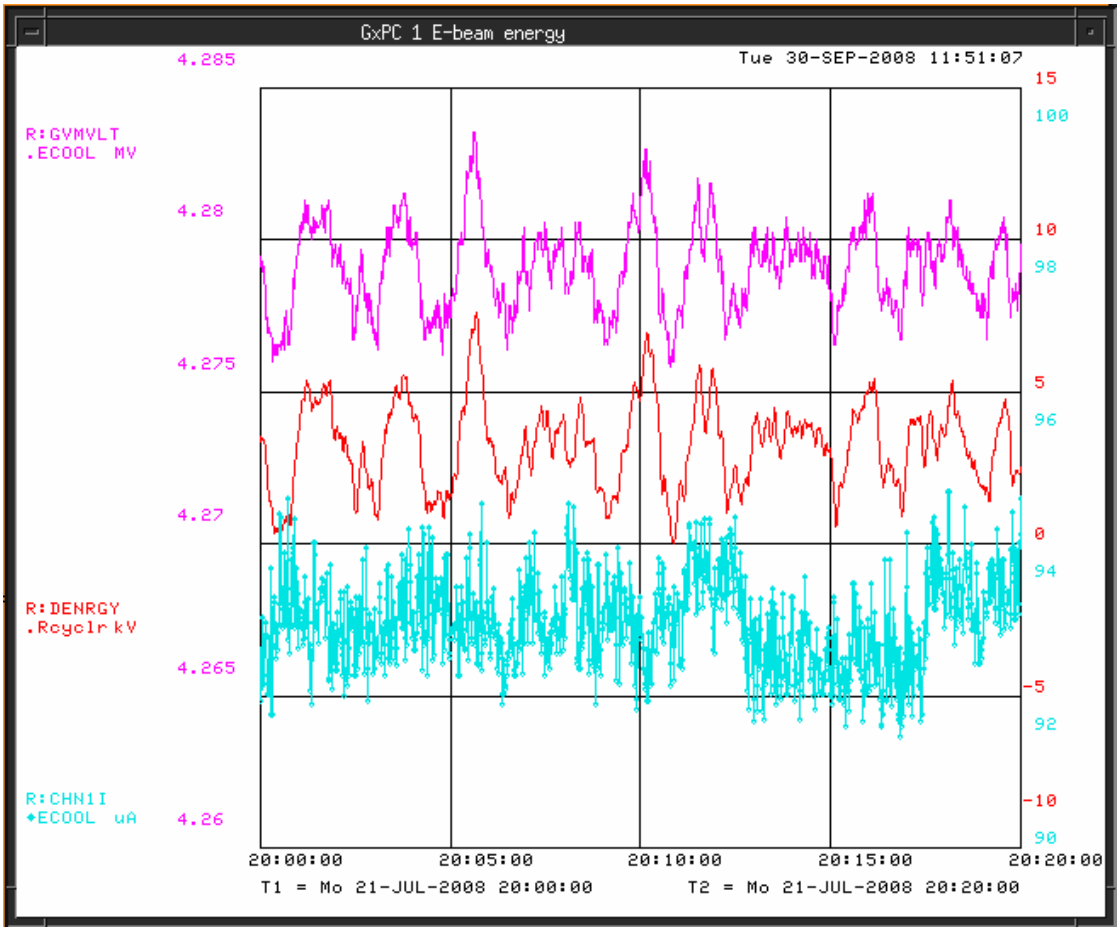

Figure 6.3. Example of energy regulation with adjusting the chain current only. July 21, 2008. The data are recorded at 1 Hz. The red curve is the beam – based energy deviation parameter, and the magenta curve shows the GVM reading (5 kV/div for both). The cyan curve is the chain current (10 μA/div),

SUMMARY

The results described in the paper reflect an 8-year experience of operating a Pelletron that generates an electron beam in the Fermilab electron cooler. The electron energy stability was found to be one of the critically important parameters of the cooler and was studied and improved during these years following the growing demand for stronger electron cooling. One of the main tools for studying the energy stability was the analyses of the electron beam position in a high-dispersion area.

The standard Pelletron high voltage regulation system was found to meet the energy stability restrictions required for effective electron cooling, suppressing the energy ripple below 150 eV rms in the bandwidth above 0.2 Hz. The ripple comes from the chain current fluctuations at the chain rotation frequency of 1.8 Hz and its harmonics.

Several mechanisms responsible for the energy drift were identified:

- Temperature sensitivity of the Generation Volt Meter's (GVM) preamplifier of 500 eV/K. Presently, its temperature is stabilized within ±0.5 K. In addition, a dedicated software loop is used to adjust the high voltage set point in accordance with the value of the energy error reconstructed from the beam trajectory.
- Dependence of the GVM reading on the Pelletron tank temperature at the rate of 400 eV/K. In a steady state, the tank temperature is kept within ±0.2 K, and the heat-up time is shortened to 4 hours by turning off SF6 cooling during that time. In addition, one can use the software loop mentioned right above to maintain a constant energy.
- The chain current drift or slow fluctuations of the corona current change the terminal voltage at the rate of 100 eV/μA. This effect was alleviated by implementation of a software loop which adjusts the chain current based on the difference between the terminal voltage set point and the GVM reading.
- The GVM reading changes with the SF6 pressure at the rate of ~500 eV/psi because of the SF6 permittivity. This effect is corrected according to the beam-based measurements of the energy error.

In addition, GVM readings can be affected by unevenness of the GVM rotation, caused by mechanical problems, and by a corona current emitted from the terminal to the GVM blades. These explanations were considered for infrequent energy down jumps at a constant GVM reading.

Most of the time, the electron energy is kept within ± 500 eV from its optimum value. The Pelletron works very reliably, and in a five year period there were no problems related to the high voltage regulation system. Even over the last year, when there were 5 problems with the system, the total downtime was about 130 hours, or less than 2% of the running time.

Parallel efforts to improve temperature stability and to add diagnostics and software regulations have proved to be prudent, helping to provide effective and reliable electron cooling.

ACKNOWLEDGMENTS

The authors are thankful to many people at Fermilab whose dedicated work made possible the reliable operation of the Electron cooler. In part, prompt and effective correction of mechanical problems would be impossible without R. Kellet, J. Nelson, F. Juarez and other technical specialists under the guidance of L. Valerio, K. Williams, and, at the R&D stage, J. Leibfritz. J. Simmons took part in all electronics repairs. In addition to contributions mentioned in the References, we acknowledge the participation of M. Sutherland for several measurements and always useful discussions with H. Pfeffer.

REFERENCES

1. G.I. Budker, Sov. Atomic Energy, Vol. 22 (1967), p. 346.
2. G.I. Budker et al., IEEE Trans. Nucl. Sci., NS-22 (1975) p. 2093.
3. I. N. Meshkov, Phys. Part. Nucl., 25 (6), p. 631 (1994).
4. S. Nagaitsev et al.,Phys. Rev. Lett. **96**, 044801 (2006)
5. L.R. Prost et al., in Proc. of COOL'07, Bad Kreuznach, Germany, September 10-14, 2007, http://cool07.gsi.de/contribution/talks#MOM1
6. Pelletrons are manufactured by the National Electrostatics Corporation (NEC), www.pelletron.com.
7. J.BSchroeder, S.J.Lunsrtrum, J.R. Adney, S.H.Phillips and R.D.Rathmell, Nuclear Instruments and Methods in Physics Research B56 (1991)
8. Improvement of the stability of the VERA accelerator, by A. Priller, R. Golser, W.Rom, and P. Steier, Proc. of SNEAP'1999, Oak Ridge, October 25-28, 1999, pp.5-9
9. Accelerator Terminal Voltage Stability, by J.A Ferry, J.J. Kolonko, S.H. Phillips and S.J.Lundstrum, Nuclear Instruments and Methods in Physics Research B64 (1992) 309-312.
10. J. Ramian, private communication about operation experience of UCSB FEL (http://sbfel3.ucsb.edu/), 1999
11. Electrostatic Accelerators, Fundamentals and Applications, edited by R. Hellborg, Springer, 2005
12. G. Kazakevich et al., Recycler Electron Cooling project: Mechanical vibrations in the Pelletron and their effect on the beam, FERMILAB-TM-2319-AD, July 2005, available at http://lss.fnal.gov/archive/test-tm/2000/fermilab-tm-2319-ad.shtml
13. Full discharges in the Fermilab Electron cooler, by L. Prost and A. Shemyakin, Proc. of COOL'05, Galena, USA, September 19-23, 2005, p. 391
14. P. W. Joireman, J. Cai, B. E. Chase and G. W. Saewert, "BPM System for Electron Cooling in the Fermilab Recycler Ring" in Beam Instrumentation Workshop 2004, AIP Conf. Proc., 732, 319 (2004).
15. Pelletron manual, NEC, 2000
16. A. Shemyakin, Summary of observations on the Pelletron charging system, Recycler group note, 2006, http://beamdocs.fnal.gov/AD-public/DocDB/ShowDocument?docid=2232

17. These programs were written and are supported by B. Kramper, L. Carmichael, and A. Warner
18. S. M. Seletskiy and A. Shemyakin, Proc. of PAC'05, Knoxville, USA, May 16-20, 2005
19. S. Nagaitsev et al., Proc. of COOL'05, Galena, USA, September 19-23, 2005, p. 39
20. The data were recorded on May 5, 2008 by P. Joireman using a dedicated program
21. A. Burov, BPM Noise Analysis, report at the Recycler departmental meeting, May 21, 2008, available at http://beamdocs.fnal.gov/AD-public/DocDB/ShowDocument?docid=3099
22. The SF6 temperature regulation was implemented by T. Butler.
23. The effect was pointed out to us by H. Pfeffer.
24. http://www.beyondchem.com/sf6.htm

Appendix A.
List of abbreviations used in the paper

CPO	Capacitive Pick-Out
BPM	Beam Position Monitor
GVM	Generation Volt Meter
HV	High Voltage
MI	Main Injector
NEC	National Electrostatic Corporation
rms	Root-mean-square
RF	Radio frequency
SF6	Sulfur Hexafluoride
TPS	Terminal Potential Stabilizer